

Calculation of the positron bound state with the copper atom

V. A. Dzuba, V. V. Flambaum, G. F. Gribakin, and C. Harabati

School of Physics, The University of New South Wales, Sydney 2052, Australia

(June 15, 2021)

Abstract

A new relativistic method for calculation of positron binding to atoms is presented. The method combines a configuration interaction treatment of the valence electron and the positron with a many-body perturbation theory description of their interaction with the atomic core. We apply this method to positron binding by the copper atom and obtain the binding energy of 170 meV ($\pm 10\%$). To check the accuracy of the method we use a similar approach to calculate the negative copper ion. The calculated electron affinity is 1.218 eV, in good agreement with the experimental value of 1.236 eV. The problem of convergence of positron-atom bound state calculations is investigated, and means to improve it are discussed. The relativistic character of the method and its satisfactory convergence make it a suitable tool for heavier atoms.

I. INTRODUCTION

Bound states of positrons with neutral atoms have not been detected experimentally yet. For a long time the prevailing view was that neutral atoms do not bind positrons. For example, Aronson *et al* [1] proved that positron binding to hydrogen is not possible, and Gertler *et al* [2] showed that a ground-state helium atom could not bind a positron. In a number of calculations positron binding was observed for alkalis and second column atoms [3–5]. However, important physical effects, such as virtual or real positronium (Ps) formation, were neglected in those works. As a result, the binding was largely considered as an artifact of the approximations used, or the positron bound states found were unstable against Ps emission. This situation has clearly changed now. Firstly, a many-body theory calculation by Dzuba *et al.* [6] indicated that atoms with larger dipole polarizabilities and ionization potentials greater than 6.8 eV (Ps binding energy) can bind positrons, and predicted positron binding energies for Mg, Zn, Cd and Hg. Subsequently, a number of recent calculations have shown and even proved, for a few lighter atoms, that positron-atom bound states do exist, [7–16].

For the problem of positron-atom binding the atoms should be divided into two groups: those with the ionization potential I smaller than 6.8 eV, and those with $I > 6.8$ eV. For the former the lowest fragmentation threshold of the positron-atom system is that of a positive ion and a Ps atom. Consequently, positron binding to such atoms should rather be described as binding of the Ps to the corresponding positive ion. Indeed, the ‘ion + Ps’ component in their wave function is large, as shown by the calculations for $\text{Li}-e^+$, $\text{Na}-e^+$ and $\text{He } 2^3S-e^+$ [7,9–12]. For atoms with $I > 6.8$ eV the positron-atom bound state is indeed an ‘atom + e^+ ’ system, at large positron-atom separations. However, the process of virtual Ps formation in this system is very important [6], especially when I is close to 6.8 eV. This effect makes positron-atom bound states a strongly correlated atomic system. The correlations in it are stronger than those one finds in its electron analogues, atomic negative ions. This feature makes the positron-atom bound complexes very interesting for the atomic theory. This also makes them a challenging testing ground for applications of modern numerical methods of atomic structure calculations.

The main difficulty in calculations of positron interaction with atoms comes from the strong electron-positron Coulomb attraction which leads to virtual positronium formation [6]. One can say that it gives rise to a specific short-range attraction between the positron and the atom, in addition to the usual polarizational potential which acts between a neutral target and a charged projectile [17–19]. This attraction can not be treated accurately by perturbations and some all-order technique is needed. In our earlier works [6,18,19] we used the Ps wave function explicitly to approximate the virtual Ps-formation contribution to the positron-atom interaction. The same physics may also explain the success of the stochastic variation method in positron-atom bound state calculations (see [12] and Refs. therein). In this approach the wave function is expanded in terms of explicitly correlated Gaussian functions which include factors $\exp(-\alpha r_{ij}^2)$ with interparticle distances r_{ij} . Using this method Ryzhikh and Mitroy obtained positron bound states for a whole range of atoms with both $I < 6.8$ eV (Li, Na, and $\text{He } 2^3S$), and $I > 6.8$ eV (Be, Mg, Zn, Cu, and Ag). This method is well suited for few-particle systems. Its application to heavier systems is done by considering the Hamiltonian of the valence electrons and the positron in the model potential

of the ionic core. However, for heavier atoms, e.g., Zn, the calculation becomes extremely time consuming [15], and its convergence cannot be ensured.

Another non-perturbative technique is configuration interaction (CI) method widely used in standard atomic calculations. This method has been applied to the positron-copper bound state in [16]. In this work the single-particle orbitals of the valence electron and positron are chosen as Slater-type orbitals, and their interaction with the Cu^+ core is approximated by the sum of the Hartree-Fock and model polarization potentials. The calculation shows slow convergence with respect to the number of spherical harmonics included in the CI expansion, $L_{\max} = 10$ being still not sufficient to extrapolate the results reliably to $L_{\max} \rightarrow \infty$.

In the present work we calculate the ground states of $\text{Cu}-e^+$ and Cu^- systems using a CI calculation within a spherical cavity of finite radius R . This procedure facilitates the convergence of the CI expansion in the difficult positron-atom case, and we show how to extrapolate the results to the $R \rightarrow \infty$ limit. The CI method which we use is based on the combined relativistic configuration interaction and many-body perturbation theory method (CI+MBPT) developed in our earlier work [20] for precise calculations of many-electron atoms with more than one valence electron. It was shown there that correlations between the core and valence electrons are very important and often contribute more to the energy than the correlations between the valence electrons. The core-valence correlations are included into the effective CI Hamiltonian of valence electrons by means of many-body perturbation theory. This allows us to achieve high accuracy in calculations of atomic energies and transition amplitudes. In the present work we adapt this approach to the positron problem.

As a single-particle basis for the CI calculations we use B -splined [21] Hartree-Fock wave functions in the cavity of finite radius R . The B -spline technique has been successfully used in atomic calculations for many years (see, e.g., review [22]) and has been recently incorporated with the CI+MBPT method [23]. The use of B -splines ensures good convergence of the CI calculation with respect to the number of radial orbitals. Convergence is further controlled by varying the cavity radius, while the effect of a finite cavity size on the energy of the system is taken into account analytically.

We have chosen the copper atom for the positron bound-state calculations for several reasons. First, this atom looks like a good candidate for positron-atom bounding. It has a large polarizability of 40 a.u. [24], and its ionization potential $I = 7.724$ eV [25] is not too far from the Ps binding energy of 6.8 eV, which ensures a sizable contribution of virtual Ps to the positron-atom attraction. Second, copper has a relatively simple electronic structure with only one valence electron above closed shells. This makes the positron-copper problem effectively a two-particle problem well suited for application of the CI+MBPT method. Third, there are accurate experimental data and a number of calculations for the energy of the copper negative ion. Thus, we can test our method on Cu^- and compare the results with those obtained by other techniques. Last but not least, the existence of the positron-copper bound state was predicted by Ryzhik and Mitroy [13] in the framework of the stochastic variational method, which allows us to compare the results obtained with the two different techniques.

II. METHOD OF CALCULATION

A. Effective Hamiltonian

We use the relativistic Hartree-Fock method in the V^{N-1} approximation to obtain the single-particle basis sets of electron and positron orbitals and to construct an effective Hamiltonian. The main point for this choice is the simplicity of the MBPT, as discussed in Ref. [20]. The self-consistent potential is determined for the Cu^+ ion and the single-particle states of the external valence electron and the positron are calculated in the field of the frozen core.

The two-particle electron-positron wave function is given by the CI expansion,

$$\Psi(\mathbf{r}_e, \mathbf{r}_p) = \sum_{i,j} C_{ij} \psi_i(\mathbf{r}_e) \phi_j(\mathbf{r}_p), \quad (1)$$

where ψ_i and ϕ_j are the electron and positron orbitals respectively. The expansion coefficients C_{ij} are to be determined by the diagonalization of the matrix of the effective CI Hamiltonian acting in the Hilbert space of the valence electron and the positron,

$$\begin{aligned} H_{\text{eff}}^{\text{CI}} &= \hat{h}_e + \hat{h}_p + \hat{h}_{ep}, \\ \hat{h}_e &= c\alpha\mathbf{p} + (\beta - 1)mc^2 - \frac{Ze^2}{r_e} + V_d^{N-1} - \hat{V}_{\text{exch}}^{N-1} + \hat{\Sigma}_e, \\ \hat{h}_p &= c\alpha\mathbf{p} + (\beta - 1)mc^2 + \frac{Ze^2}{r_p} - V_d^{N-1} + \hat{\Sigma}_p, \\ \hat{h}_{ep} &= -\frac{e^2}{|\mathbf{r}_e - \mathbf{r}_p|} - \hat{\Sigma}_{ep}, \end{aligned} \quad (2)$$

where \hat{h}_e and \hat{h}_p the effective single-particle Hamiltonians of the electron and positron, and \hat{h}_{ep} is the effective electron-positron two-body interaction. Apart from the relativistic Dirac operator, \hat{h}_e and \hat{h}_p include the direct and exchange Hartree-Fock potentials of the core electrons, V_d^{N-1} and V_{exch}^{N-1} , respectively. The additional $\hat{\Sigma}$ operators account for correlations involving core electrons (see [20] for a detailed discussion). We calculate $\hat{\Sigma}$ using the second-order MBPT in the residual Coulomb interaction. $\hat{\Sigma}_e$ describes the interaction between the valence electron and the electrons of the core. All four second-order diagrams for the $\hat{\Sigma}_e$ are presented in Fig. 1. $\hat{\Sigma}_p$ is the correlation interaction between the positron and the core. In the second-order $\hat{\Sigma}_p$ is represented by a sole diagram in Fig. 2. Both operators are often called correlation *potentials*, because these *non-local* operators can be included into the equations for the single-particle orbitals together to the Hartree-Fock potential. $\hat{\Sigma}_e$ and $\hat{\Sigma}_p$ are energy-dependent operators, which are different for the electron and the positron. They are calculated separately for each partial wave, ($s_{1/2}$, $p_{1/2}$, $p_{3/2}$, etc.). However, at large distances both operators have the same asymptotic behaviour,

$$\Sigma_e(\mathbf{r}, \mathbf{r}'), \quad \Sigma_p(\mathbf{r}, \mathbf{r}') \simeq -\frac{\alpha e^2}{2r^4} \delta(\mathbf{r} - \mathbf{r}'), \quad (3)$$

where α is the dipole polarizability of the atomic core. This asymptotic form comes from the dipole contribution of the first diagram in Fig.1 for the electron, and diagram in Fig.2 for the positron. Formula (3) with some empirical cut-off at small distances is often used as an approximation for the correlation potentials, and is usually called ‘polarization potential’.

$\hat{\Sigma}_{ep}$ is another type of correlations between the external particles and and core electrons. It can be described as screening of Coulomb interaction between the external electron and positron by the core electrons. There are in all six second-order diagrams for $\hat{\Sigma}_{ep}$. Three of them are shown in Fig. 3. The other three can be obtained from them by mirror reflection with respect to the vertical axis. When the electron and the positron are well outside the atomic core $\hat{\Sigma}_{ep}$ is given by the following asymptotic expression,

$$\Sigma_{ep}(\mathbf{r}_e, \mathbf{r}_p) \simeq \frac{\alpha e^2 \mathbf{r}_e \cdot \mathbf{r}_p}{r_e^3 r_p^3}. \quad (4)$$

Similarly to Eq. (3), this formula is often used to construct rough approximations for $\hat{\Sigma}_{ep}$. Such potentials are called ‘di-electronic correction’, or ‘two-body polarization potential’.

Diagrammatic expansions in Figs. 1, 2 and 3 enable one to include valence-core correlations in an *ab initio* manner. To increase the accuracy of the calculations higher-order contributions to $\hat{\Sigma}$ can be taken into account effectively, by introducing a numerical factor before $\hat{\Sigma}$. For example, the coefficient for $\hat{\Sigma}_e$ can be chosen by fitting the energies of the neutral atom states to the experimental data. In doing so the important non-local structure of the operators is preserved.

B. Basis set

We use *B*-spline basis functions [21] to calculate the diagrams for $\hat{\Sigma}$ and to construct the single-particle orbitals for the CI expansion (1). For this purpose the atomic system is confined to a cavity of radius R , and the wave functions are set to zero at $r = R$. For a sufficiently large R the error introduced by this boundary condition is very small for atomic-size binding energies, $\sim \exp(-2\kappa R)$, where κ is related to the binding energy as $\epsilon_B = \kappa^2 \hbar^2 / 2m$. However, for weakly bound states, e.g. those of the positron with the atom, this error has to be considered more carefully (see below). The interval $[0, R]$ is divided into a number of segments and *B*-splines are constructed on them as piecewise polynomials of a certain degree. They are bell-shaped overlapping smooth functions. With an appropriate choice of the radial mesh they can approximate atomic wave functions to a very high precision. Note that it is not convenient to use *B*-splines directly in CI or MBPT calculations because of their non-orthogonality. Instead, we use their linear combinations which are eigenstates of the single-particle Hartree-Fock Hamiltonian. This ensures orthogonality, allows to separate core and valence states and improves convergence, since only a relatively small number of lower Hartree-Fock eigenstates are sufficient for the convergence of the CI calculation. This also means that while we use the same *B*-splines for the electron and positron states the resulting single-particle basis states are different, because the Hartree-Fock Hamiltonians for the electrons and positrons are different. Another advantage of the use of *B*-splines is that the convergence can be controlled by the cavity radius R (its reduction leads to a more rapid convergence), while its effect on the energy is taken into account analytically.

C. Effect of finite cavity size

The choice of the cavity radius R (see above) is dictated by a compromise between the convergence rate and the required accuracy of the calculations. On one hand, the radius must be large enough to accommodate the wave function of the state under investigation, e.g., the positron-atom bound state. On the other hand, smaller radii mean faster convergence, both with respect to the number of radial orbitals and, which is especially important for positron-atom calculations, to the number of angular harmonics. This effect is very strong since convergence is determined by the cavity volume which is proportional to R^3 , and having a smaller radius means that one needs fewer basis states to describe the wave function.

The problem of convergence is crucial for the positron-atom interaction. As discussed in the Introduction, the positron tends to form virtual Ps with the external atomic electron [6,17,18]. The positronium radius $r_{\text{Ps}} \sim 2a_0$ can be small compared to the characteristic size of the positron-atom bound state wave function, $r \sim 1/\kappa \gg a_0$, where a_0 is the Bohr radius. To describe Ps at large separations from the atom expansion (1) needs to be extended to very high values of angular momentum L and principal quantum number n to account accurately for the virtual Ps formation. This problem is well known in positron-atom scattering calculations, see e.g. [26]. Smaller cavity radii force virtual Ps to be at smaller distances, thereby improving the convergence significantly. However the energy of the system is affected. Therefore, the convergence and the accuracy of the calculation can be really improved only if the effect of a finite-radius cavity on the energy is taken into account.

To consider the effect of cavity on the energy of the system let us consider the problem of a particle weakly bound in an s state by a finite-range potential. ‘Weakly bound’ here means that the binding energy is much smaller than the typical scale of the potential. This is definitely true for positron-atom bound states whose binding energy is much smaller than 1 eV. To determine the radial wave function $\chi(r)$ at large distances it is sufficient to impose on it a boundary condition

$$\left. \frac{1}{\chi} \frac{d\chi}{dr} \right|_{r=a} = -\kappa, \quad (5)$$

at the outer radius $r = a$ of the potential well [27]. The κ parameter is related to the energy of the bound state $\varepsilon = -\kappa^2 \hbar^2 / 2m$, and determines the asymptotic form of the wave function, $\chi(r) \simeq Ae^{-\kappa r}$.

The boundary condition is unchanged when we place the system in the cavity of finite radius R , $R > a$, provided the energy of the bound state is still small. However, the wave function must now turn into zero at the cavity radius, $\chi(R) = 0$. This shifts the energy of the weakly bound state up from ε to some other value ε_R , which depends on the radius of the cavity. The Schrödinger equation for $a < r < R$, where the potential is vanishingly small, is

$$\frac{\hbar^2}{2m} \frac{d\chi^2}{dr^2} + \varepsilon_R \chi(r) = 0, \quad (6)$$

After solving it with boundary conditions (5) and $\chi(R) = 0$, one obtains a negative eigenvalue, $\varepsilon_R = -\kappa_R^2 \hbar^2 / 2m$, where

$$\kappa = \kappa_R / \tanh[\kappa_R(R - a)], \quad (7)$$

if R is not too small, $R - a > \kappa^{-1}$. As one can see, for $R \rightarrow \infty$ the solution of Eq. (7), κ_R , approaches its asymptotic value κ , and the energy in the cavity $\varepsilon_R \rightarrow \varepsilon$. For a smaller cavity radius the eigenvalue becomes positive, $\varepsilon_R = k_R^2 \hbar^2 / 2m$, where k_R is found from

$$\kappa = k_R / \tan[k_R(R - a)]. \quad (8)$$

This means that the state which is bound may appear as unbound due to the effect of the cavity. Equation (8) is valid for $k_R(R - a) < \frac{\pi}{2}$. Otherwise, $\kappa < 0$, and the energy is too high, so that it remains positive even when the cavity wall is removed.

Equations (7) and (8) can be used to find the infinite-cavity energy $\varepsilon = -\kappa^2 \hbar^2 / 2m$ from the energy ε_R calculated for the finite cavity radius R . It is important that these formulae are insensitive to the detailed shape of the atomic potential, and depend only on the atomic radius a . The value of a can be estimated from the position of the classical turning point r_c , in the potential for an external atomic electron,

$$\frac{e^2}{r_c} = I = \frac{e^2}{2a_0\nu^2},$$

where ν is the effective quantum number of the valence electron. Beyond the turning point the valence electron's wave function decreases exponentially, as $\exp(-r/a_0\nu)$. Therefore, a reasonable estimate for is

$$a = r_c + a_0\nu = (2\nu^2 + \nu)a_0 \quad (9)$$

For copper ($I = 0.28349$ a.u., $\nu = 1.33$) this gives $a \approx 5a_0$. A more accurate value of a can be found by applying Eq. (7) to two bound-state calculations performed with two different cavity radii R . The uncertainty in the value of a is in fact unimportant, as long as we consider weakly bound states for which $\kappa a \ll 1$.

Note that the wave function is also affected by the finite cavity size. This should be taken into account in calculations of the annihilation rate and other matrix elements. The annihilation rate is proportional to the probability of finding the positron close to the atom. For $a \ll R$ the wave function at $r \lesssim a$ is affected via normalization only. The change of the normalization can be found by comparing the normalization integral for $r > a$ calculated numerically within the cavity,

$$\int_a^R \chi^2(r) dr ,$$

with the analytical value

$$\int_a^\infty e^{-2\kappa r} dr = \frac{1}{2\kappa} e^{-2\kappa a}.$$

III. RESULTS AND DISCUSSION

A. Copper negative ion

To test the method and find out what accuracy can be achieved we first apply it to the copper negative ion. This is an effective two-particle problem technically very similar to the positron-copper interaction considered above. It should be mentioned that for Cu^- only the electron $\hat{\Sigma}$ -operator is involved (Fig. 1), and for the screening of the electron-electron interaction, instead of the diagrams on Fig. 3, one must use similar diagrams presented in [20] (Fig.4). The results of calculations for Cu and Cu^- are presented in table I together with the experimental values. The energies are given with respect to the Cu^+ core. The accuracy of the Hartree-Fock approximation is very poor. The binding energy of the $4s$ electron in neutral Cu is underestimated by about 20%, while the negative ion Cu^- appears altogether unbound (its energy lies above that of the neutral atom). The inclusion of core-valence correlations ($\hat{\Sigma}$) does improve the energy of the neutral atom, but the negative ion is still not bound. The standard CI method, in contrast, takes into account the valence-valence correlations, while neglecting the core-valence correlations. It does produce binding for the negative ion, but the binding energy is almost two times smaller than the experiment value. Only when both core-valence and valence-valence correlations are included the accuracy improves significantly. It is equal to 2.6% for the ionization potential of the neutral atom and 10% for the electron affinity, which is quite good for a relatively simple *ab initio* calculation. The remaining discrepancy is mostly due to third and higher-order correlation corrections in $\hat{\Sigma}$, since the configuration expansion for Cu^- converges rapidly, and the corresponding error is small.

To simulate the effects of higher-order terms in $\hat{\Sigma}$ and thus further improve the accuracy of calculations we introduce numerical factors before the $\hat{\Sigma}_e$ operators to fit the lowest s , p and d energy levels of the neutral copper atom. These factors are $f_s = 1.17$, $f_p = 1.42$ and $f_d = 1.8$ in the s , p and d channels, respectively. Table I shows that these factors also significantly improve the calculated electron affinity. It is natural to assume that the same procedure should work equally well for the positron-atom problem.

Results of other calculations of the electron affinity of copper are presented in table II. Note that only a coupled-cluster (CC) method produces a result more accurate than ours. It is interesting to mention among other results the results by Mitroy and Ryzhikh [13,16] who calculated Cu^- for the same purpose as we do, i.e., to gauge the accuracy of their method for the positron-atom problem. Their first result for electron affinity to copper, 0.921 eV, was obtained by the stochastic variational method, while another result 0.916 eV was achieved in the standard CI calculation. Both methods are variational in nature and differ basically by the form of the trial two-electron wave function. Since the two results agree well with each other, good convergence has probably been achieved in both methods. However there is a noticeable discrepancy between their result and the experimental electron affinity value. From our point of view the most probable source of this discrepancy is approximate treatment of the $\hat{\Sigma}$ operator of the valence-core interaction. In their works Mitroy and Ryzhikh use approximate expressions for the core polarization potentials, based on asymptotic formulae (3) and (4), which include only dipole core polarization in the local energy-independent form. Note again that the actual $\hat{\Sigma}$ operator is energy dependent. It is

different for different angular momenta, and for the electron and positron, while approximate expression (3) is always the same. Note also that the screening operator $\hat{\Sigma}_{ep}$ depends not only on the states involved but also on the multipolarity of the Coulomb integral. Approximate formula (4) describes the dipole part of screening only, however, other Coulomb multipoles are also screened. Even though the largest contribution to screening comes from the dipole term, monopole and quadrupole screening can not be neglected. For example, monopole screening directly contributes to the diagonal Hamiltonian matrix elements in important configurations like $4s^2$ in Cu^- , while dipole screening affects only the off-diagonal matrix elements.

B. Positron binding to copper

The binding energy of Cu^- is about 0.045 a.u. It corresponds to a bound-state parameter $\kappa \approx 0.3$, and the cavity does not have a noticeable effect on the calculated energies of Cu^- , let alone Cu . The relative error introduced by the cavity can be easily estimated from Eq. (7), and even for a moderate $R = 15a_0$ it does not exceed 0.1% for the electron affinity.

For the positron bound state the situation is different. As indicated by the calculation of Ref. [13], the κ value for the $\text{Cu}-e^+$ bound state is about 0.1. This is why we have performed the calculation of the positron-atom bound state using two different cavity radii, $R = 15a_0$ and $R = 30a_0$, to make sure that convergence is really achieved. The convergence pattern with respect to the number of basis states used is illustrated in Figs. 4 and 5. Both plots show the energy of the electron-positron pair moving in the field of Cu^+ , with respect to the energy of the Cu^+ ion (in atomic units). Empty circles correspond to $R = 15a_0$, while solid ones correspond to $R = 30a_0$. Dashed line shows the ground-state energy of the neutral copper atom. The positron-atom state is bound when its energy is below the dashed line. Fig. 4 shows the electron-positron energy of $\text{Cu}-e^+$ as a function of the number of radial basis functions in each electron and positron partial wave, n . The total number of partial waves is fixed by $L_{\max} = 10$. Note that convergence is visibly faster for the smaller cavity radius. For $R = 15a_0$ saturation begins at $n \approx 10$ while for $R = 30a_0$ the same level of saturation can be seen only at $n \approx 18$. Fig. 5 shows the $\text{Cu}-e^+$ energy as a function of the number of partial waves included, while the number of radial wave functions in each wave is fixed at $n = 16$ for $R = 15a_0$ and $n = 22$ for $R = 30a_0$. Saturation can be clearly achieved for both radii at $L_{\max} \gtrsim 10$. The difference in energy at the last (lowest) points for $R = 15a_0$ and $R = 30a_0$ in both figures is the effect of a finite cavity radius. It shifts the energy obtained in the $R = 15a_0$ calculation up with respect to the $R = 30a_0$ result. This effect can be easily taken into account using the formulae presented in section II C. It turns out that the results for both cavity radii coincide, i.e., yield identical κ from Eq. (7), for the atomic potential radius of $a = 5.5a_0$. The final binding energy obtained is 0.0062 a.u., or 170 meV. This should be compared to the result of Ryzhikh and Mitroy [13], which is 0.005518 a.u. or 150 meV. From the discussion of the accuracy of calculations which follows we conclude that the difference between two results is within the accuracy of both methods. A similar value is achieved in the CI calculation [16], which used 14 radial orbitals in each partial wave up to $L_{\max} = 10$, after extrapolation to $L_{\max} = \infty$. However, the latter procedure has considerable uncertainties.

There are several factors which affect the accuracy of our calculations.

- The accuracy of calculation of $\hat{\Sigma}$ and contributions of higher-order correlations. This can be estimated by comparing calculations with and without the fitting parameters, as discussed in section III A. The introduction of the fitting parameters for the electron part of the correlation operator $\hat{\Sigma}_e$ reduces the binding energy by about 0.0009 a.u. However, the relevant uncertainty must be considerably smaller. Firstly, we saw that the use of fitting parameters really improves the calculated electron affinity of copper. We should expect the same effect for the positron binding energy. Secondly, the effects of the fitting parameters on the electron and positron operators $\hat{\Sigma}_e$ and $\hat{\Sigma}_p$ largely cancel each other.
- Incompleteness of the basis set. We have seen from Figs 4 and 5 that the level of convergence achieved is very high and the corresponding uncertainty is small. Nevertheless, there is a hidden uncertainty related to the radial coordinate mesh used, the number of splines and other parameters which determine the details of the numerical procedure. Varying these parameters shows that their effect on the binding energy does not exceed 0.001 a.u., when estimated conservatively.
- Finite cavity radius. This effect on the binding energy calculated at $R = 30a_0$ is very small (~ 0.0001 a.u.). Since the results for $R = 15a_0$ and $R = 30a_0$ coincide for very reasonable value of the positron-atom potential radius $a = 5.5a_0$, it is reasonable to believe that the corresponding uncertainty is very small too.

Note that the difference between our calculated electron affinity of copper and the experimental value is 0.00066 a.u. If this value is compared with the numbers presented above, it is evident that it also gives a reasonable estimate of the accuracy of the calculation of the positron-copper binding energy (about 10%). Since the accuracy of calculations by Mitroy and Ryzhikh [13] is not discussed in their paper the only thing we can do to estimate it is to use the same approach. Their best result for Cu^- differs from the experimental value by 0.0116 a.u. (20% of the positron binding energy). If we adopt this value as the uncertainty of their result for the positron binding by copper, we see that the two results for $\text{Cu}-e^+$ bound state agree with each other within the accuracy of the methods.

REFERENCES

- [1] I. Aronson, C. J. Kleinman and L Spruch, Phys. Rev. A **4**, 841 (1971).
- [2] F. H. Gertler, H. B. Snodgrass, and L. Spruch, Phys. Rev. **172**, 110 (1968).
- [3] D. C. Clary, J. Phys. B **9**, 3115 (1976).
- [4] S. J. Ward, M. Horbatsch, R. P. McEachran, and A. D. Stauffer, J. Phys. B **22**, 3763 (1989).
- [5] R. Szmytkowski, J. Phys. II France **3**, 183 (1993); R. Szmytkowski, Acta Physica Polonica A **84**, 1035 (1993).
- [6] V. A. Dzuba, V. V. Flambaum, G. F. Gribakin, and W. A. King, Phys. Rev. A **52**, 4541 (1995).
- [7] G. G. Ryzhikh and J. Mitroy, Phys. Rev. Lett. **79**, 4124 (4124).
- [8] K. Strasburger and H. Chojnacki, J. Chem. Phys. **108**, 3218 (1998).
- [9] G. G. Ryzhikh and J. Mitroy, J. Phys. B. **31**, L265 (1998); **31** 3465 (1998);
- [10] J. Yuan, B. D. Esry, T. Morishita, and C. D. Lin, Phys. Rev. A **58**, R4 (1998).
- [11] G. G. Ryzhikh and J. Mitroy, J. Phys. B. **31**, L401 (1998).
- [12] G. G. Ryzhikh, J. Mitroy and K. Varga, J. Phys. B. **31**, 3965 (1998).
- [13] G. G. Ryzhikh and J. Mitroy, J. Phys. B. **31**, 4459 (1998).
- [14] G. G. Ryzhikh and J. Mitroy, J. Phys. B. **31**, 5013 (1998).
- [15] J. Mitroy and G. G. Ryzhikh, J. Phys. B. **32**, 1375 (1999).
- [16] J. Mitroy and G. G. Ryzhikh, J. Phys. B. **32**, 2831 (1999).
- [17] V. A. Dzuba, V. V. Flambaum, W. A. King, B. N. Miller, and O. P. Sushkov, Phys. Scripta T **46**, 248 (1993).
- [18] G. F. Gribakin and W. A. King, J. Phys. B **27**, 2639 (1994).
- [19] V. A. Dzuba, V. V. Flambaum, G. F. Gribakin, and W. A. King, J. Phys. B **29**, 3151 (1996).
- [20] V. A. Dzuba, V. V. Flambaum, and M. G. Kozlov, Phys. Rev. A **54**, 3948 (1996).
- [21] C. deBoor, *A Practical Guide to Splines* (Springer, New York, 1978).
- [22] J. Sapirstein and W. R. Johnson, J. Phys. B **29**, 5213 (1996).
- [23] V. A. Dzuba and W. R. Johnson, Phys. Rev. A **57**, 2459 (1998).
- [24] A. A. Radtsig and B. M. Smirnov, *Parameters of Atoms and Atomic Ions: Handbook* (Energoatomizdat, Moscow, 1986); *CRC Handbook of Physics and Chemistry*, 69th edition, Editor-in Chief R. C. Weast (Boca Raton, Florida, CRC Press, 1988).
- [25] C. E. Moore, *Atomic Energy Levels*, Natl. Bur. Stand. Circ. No. 467 (U.S. GPO, Washington, DC, 1958), Vol. III.
- [26] I. Bray and A. Stelbovics, Phys. Rev. A **48** 4787 (1993).
- [27] L. D. Landau and E. M. Lifshitz, *Quantum Mechanics*, 3rd ed. (Pergamon Press, Oxford, UK, 1977).
- [28] C. W. Bauschlicher Jr., S. P. Walch, and H. Partridge, Chem. Phys. Lett. **103**, 291 (1984).
- [29] C. M. Marian, Chem. Phys. Lett. **173**, 175 (1990).
- [30] P. Schwerdtfeger and G. A. Bowmaker, J. Chem. Phys. **100**, 4487 (1994).
- [31] P. Neogrady, V. Kello, M. Urban, and A. J. Sadrej, Int. J. Quantum Chem. **63**, 557 (1997).
- [32] H. Hotop and W. C. Lineberger, J. Phys. Chem. Ref. Data **14**, 731 (1975).
- [33] R. C. Bilodeau, J. Phys. B, 3885 (1998).

TABLES

TABLE I. Ground state energies of Cu and Cu⁻ calculated using different approximations (a.u.).

	Cu	Cu ⁻	Electron affinity
RHF ^a	-0.23830	-0.20309	-0.03521
RHF + Σ ^b	-0.27672	-0.27280	-0.00392
CI ^c	-0.23830	-0.26424	0.02594
CI + Σ ^d	-0.27672	-0.31802	0.04130
CI + $f \times \Sigma$ ^e	-0.28394	-0.32869	0.04475
Experiment ^f	-0.28394	-0.32935	0.04541

^aRelativistic Hartree-Fock; a single-configuration approximation, no core-valence correlations are included.

^bSingle-configuration approximation, core-valence correlations are included by means of MBPT.

^cStandard CI method.

^dCI+MBPT method, both core-valence and valence-valence correlations are included.

^e Σ for *s*-wave is taken with factor $f = 1.18$ to fit the Cu ground state energy.

^fReferences [25,33].

TABLE II. Electron affinities of Cu (eV). Comparison with other calculations and experiment.

Affinity	Ref.	Method
Theory		
1.06	[28]	Nonrelativistic MR CI calculations
1.01	[29]	MR CI calculations in the DK no-pair formalism
1.199	[30]	
1.236	[31]	Relativistic coupled cluster method
0.921	[13]	Nonrelativistic stochastic variational method
0.916	[16]	Nonrelativistic CI method
1.218		Present work
Experiment		
1.226	[32]	
1.2358	[33]	

FIGURES

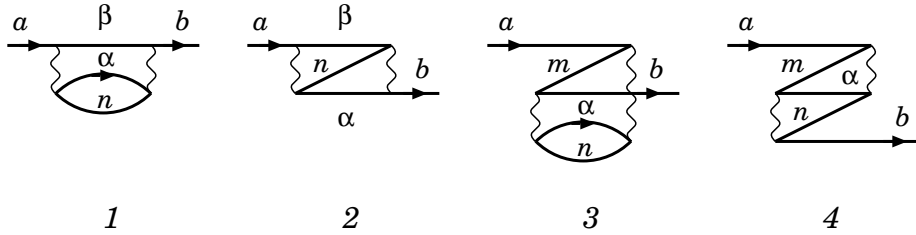


FIG. 1. Second-order diagrams for the self-energy of the valence electron ($\hat{\Sigma}_e$ operator). Summation of excited electron states α and β and core hole states m and n is assumed.

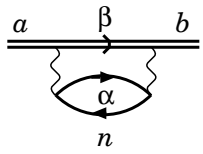


FIG. 2. Second-order diagram for the positron self-energy ($\hat{\Sigma}_p$ operator). Double line denotes positron states.

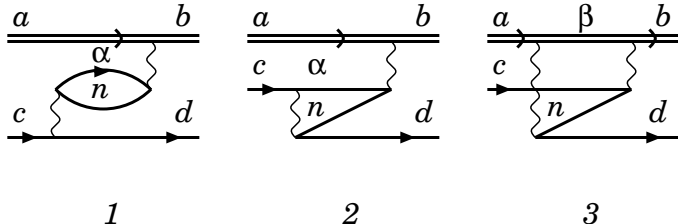


FIG. 3. Screening of the positron-electron Coulomb interaction ($\hat{\Sigma}_{ep}$ operator).

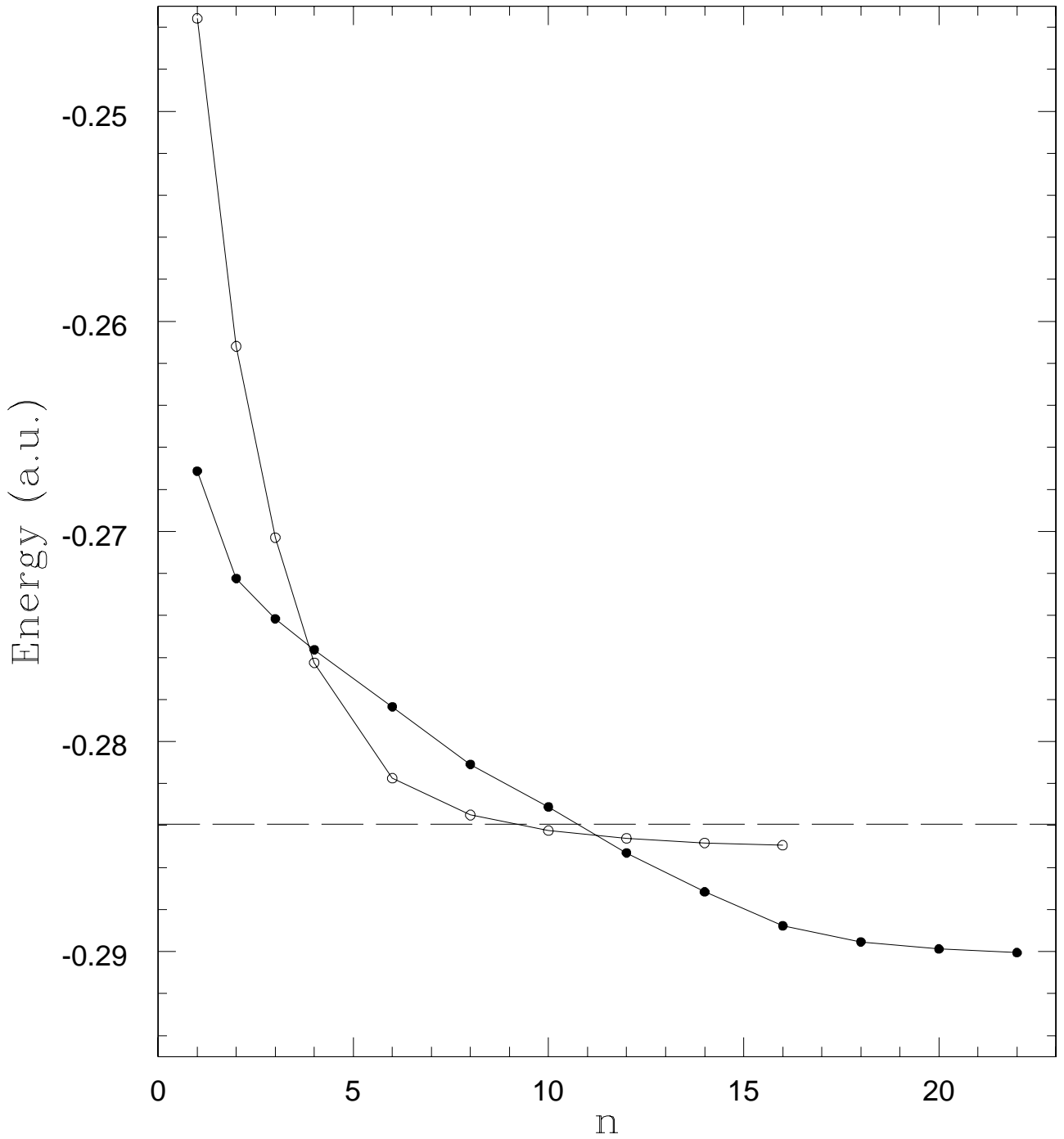


FIG. 4. Energy of $\text{Cu}e^+$ as a function of the number of radial electron and positron basis functions in each partial wave ($L_{\max} = 10$). Open circles are for $R = 15a_0$, and solid ones for $R = 30a_0$.

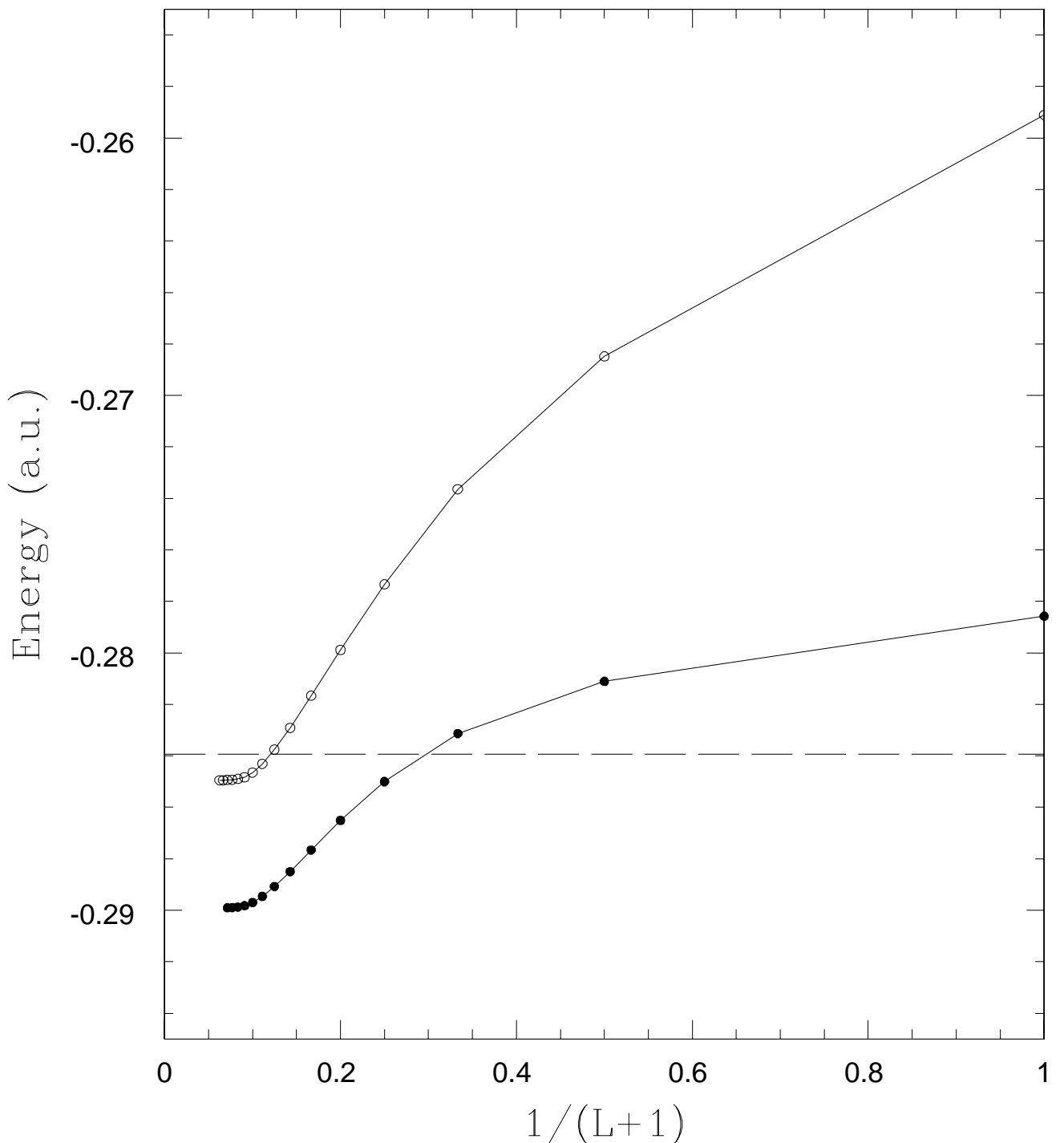


FIG. 5. Energy of $\text{Cu}e^+$ as a function of maximal orbital momentum of the electron and positron orbitals in the CI expansion. Open circles are for $R = 15a_0$, and solid ones for $R = 30a_0$.